

# Long-Term Fish Oil Supplementation Induces Cardiac Electrical Remodeling by Changing Channel Protein Expression in the Rabbit Model

Xulin Xu<sup>1</sup>, Min Jiang<sup>1</sup>, Yuhong Wang<sup>1</sup>, Timothy Smith<sup>2</sup>, Clive M. Baumgarten<sup>1,3</sup>, Mark A. Wood<sup>3</sup>, Gea-Ny Tseng<sup>1\*</sup>

**1** Department of Physiology and Biophysics, Virginia Commonwealth University, Richmond, Virginia, United States of America, **2** Department of Chemistry, University of Richmond, Richmond, Virginia, United States of America, **3** Division of Cardiology, Department of Internal Medicine, Medical College of Virginia, Richmond, Virginia, United States of America

## Abstract

Clinical trials and epidemiological studies have suggested that dietary fish oil (FO) supplementation can provide an anti-arrhythmic benefit in some patient populations. The underlying mechanisms are not entirely clear. We wanted to understand how FO supplementation (for 4 weeks) affected the action potential configuration/duration of ventricular myocytes, and the ionic mechanism(s)/molecular basis for these effects. The experiments were conducted on adult rabbits, a widely used animal model for cardiac electrophysiology and pathophysiology. We used gas chromatography - mass spectroscopy to confirm that FO feeding produced a marked increase in the content of n-3 polyunsaturated fatty acids in the phospholipids of rabbit hearts. Left ventricular myocytes were used in current and voltage clamp experiments to monitor action potentials and ionic currents, respectively. Action potentials of myocytes from FO-fed rabbits exhibited much more positive plateau voltages and prolonged durations. These changes could be explained by an increase in the L-type Ca current ( $I_{CaL}$ ) and a decrease in the transient outward current ( $I_{to}$ ) in these myocytes. FO feeding did not change the delayed rectifier or inward rectifier current. Immunoblot experiments showed that the FO-feeding induced changes in  $I_{CaL}$  and  $I_{to}$  were associated with corresponding changes in the protein levels of major pore-forming subunits of these channels: increase in Cav1.2 and decrease in Kv4.2 and Kv1.4. There was no change in other channel subunits (Cav1.1, Kv4.3, KCHIP2, and ERG1). We conclude that long-term fish oil supplementation can impact on cardiac electrical activity at least partially by changing channel subunit expression in cardiac myocytes.

**Citation:** Xu X, Jiang M, Wang Y, Smith T, Baumgarten CM, et al. (2010) Long-Term Fish Oil Supplementation Induces Cardiac Electrical Remodeling by Changing Channel Protein Expression in the Rabbit Model. PLoS ONE 5(4): e10140. doi:10.1371/journal.pone.0010140

**Editor:** Joel Gagnier, University of Toronto, Canada

**Received:** January 5, 2010; **Accepted:** March 22, 2010; **Published:** April 13, 2010

**Copyright:** © 2010 Xu et al. This is an open-access article distributed under the terms of the Creative Commons Attribution License, which permits unrestricted use, distribution, and reproduction in any medium, provided the original author and source are credited.

**Funding:** This work was supported by R21 AT0044601 from the National Center for Complementary and Alternative Medicine, and RO1 HL67840 from the National Heart, Lung, and Blood Institute of the National Institutes of Health (to G.N.T.). The funders had no role in study design, data collection and analysis, decision to publish, or preparation of the manuscript.

**Competing Interests:** The authors have declared that no competing interests exist.

\* E-mail: gtseng@vcu.edu

## Introduction

Clinical trials and epidemiological studies have suggested that dietary fish oil (FO) supplementation can provide an anti-arrhythmic benefit in some patient populations [1]. One of the largest trials, the GISSI Prevenzione trial, showed that patients that survived recent (<3 months) myocardial infarction when receiving FO supplementation had a reduced mortality rate [2]. There was no reduction in the risk for non-fatal myocardial infarction. The reduced mortality could be attributed, at least partly, to a protection against sudden cardiac death by the FO supplementation [2].

The mechanism(s) underlying the anti-arrhythmic effect of FO supplementation has been under investigation for years. It has been proposed that this anti-arrhythmic effect is mainly due to a direct suppression of Na ( $I_{Na}$ ) and L-type Ca ( $I_{CaL}$ ) currents in cardiac myocytes by the active ingredients of FO, n-3 polyunsaturated fatty acids (PUFAs), such as docosahexaenoic acid (DHA or C22:6,n-3) and eicosapentaenoic acid (EPA or C20:5,n-3) [3]. This is similar to a combination of class I and

class IV anti-arrhythmic mechanisms. There are several issues with this proposed anti-arrhythmic mechanism for fish oil or n-3 PUFAs. First, the acute current-suppressing effects observed in tissue bath experiments cannot explain why clinically it takes ~3 months for FO supplementation to manifest the protective effect [2]. Second, n-6 PUFAs (i.e. arachidonic acid) have similar current-suppressing effects in tissue bath experiments [4,5]; yet they do not provide anti-arrhythmic protection. Third, although acute exposure to DHA or EPA can suppress  $I_{Na}$  in neonatal rat cardiomyocytes [4] or in heterologous expression systems [6], experiments of feeding adult animals with an FO-rich diet for weeks have not shown any  $I_{Na}$  reduction [7].

To more closely mimic the clinical situation, it is important to study the effects of dietary FO supplementation in animal models after long-term (weeks to months) FO feeding. To gain insights into the ionic mechanisms for the anti-arrhythmic effects of FO supplementation, it is necessary to study how such treatment can impact on ion channels that are involved in shaping the action potential configuration and duration in the heart. Since clinically the protective effects of FO supplementation lag behind the

beginning of FO regimen by about 3 months [2], the involvement of changes in gene expression must be taken into consideration. Therefore, to provide a molecular basis for such changes in ion channel function, it is necessary to examine the expression level of relevant ion channel subunit proteins in cardiac myocytes.

Our goals were to understand: (a) how FO feeding for 4 weeks could affect the action potential configuration and duration in ventricular myocytes, (b) how FO feeding affected the function of ion channels that are important determinants of action potential properties, and (c) whether changes in ion channel function involved alterations in gene expression. We chose a popular animal model, rabbit, in our experiments. Rabbits have been widely used to study cardiac electrophysiology, pathology and pharmacology. Our data confirm that FO feeding induces an ‘electrical remodeling’ in rabbit ventricular myocytes by altering channel gene expression.

## Materials and Methods

### 1. Animal preparation

The investigation conforms with the *Guide for the Care and Use of Laboratory Animals* published by the US National Institutes of Health (NIH Publication No. 85-23, revised 1996). The animal protocol is

reviewed by IACUC of VCU annually (IACUC protocol # 10294). Twenty-three young adult (2–2.5 months) male New Zealand White rabbits were included in this study. Ten (FO group) were fed complete content of FO soft gel (NatureMade, ~120 mg/kg/d of DHA+EPA) for 4 weeks. The others (control group) were not given any fat supplementation. FO-fed rabbits did not show any signs of pathology. Their weight gain during 4-week FO feeding was the same as control rabbits during the same period: at the end of 4 weeks, body weights of control rabbits increased from  $2.36 \pm 0.05$  to  $2.90 \pm 0.09$  kg, while those of FO-fed rabbits increased from  $2.38 \pm 0.07$  to  $2.88 \pm 0.05$  kg ( $p > 0.05$ ). Furthermore, the FO-fed rabbits did not show any signs of myocardial hypertrophy: mean values of cell capacitance were  $160 \pm 15$  and  $159 \pm 6$  pF for control and FO myocytes ( $n = 20$  and  $33$ ,  $p > 0.05$ ).

For myocyte isolation, the aorta was cannulated and the heart was mounted on a Langendorff apparatus for enzyme treatment (see below). If the heart was used for biochemical experiments, it was dissected into different regions of  $\sim 5 \times 5$  mm chunks, snap frozen in liquid nitrogen and stored at  $-80^\circ\text{C}$  until experiments.

### 2. Single myocyte preparation

The heart was perfused retrogradely through the aorta sequentially with the following oxygenated solutions warmed to

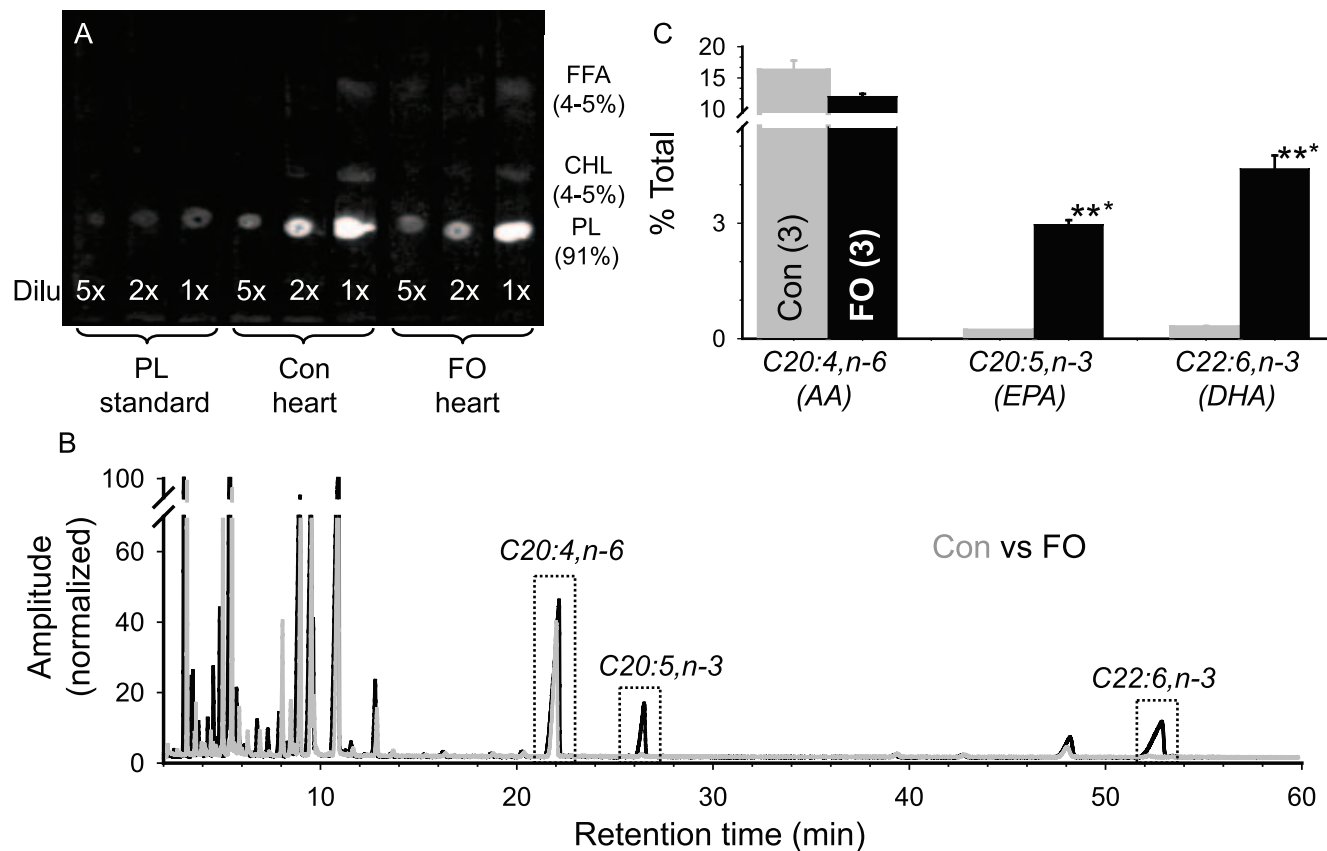


**Figure 1. Fish oil (FO) feeding increased the n-3 PUFA content in phospholipids (PLs) of rabbit hearts.** Lipids were extracted from ventricular myocardium and analyzed by thin-layer chromatography (TLC), or transmethylated followed by characterization/quantification by gas chromatography-mass spectroscopy (GC-MS). (A) Image of a representative TLC plate sprayed with 2',7'-dichlorofluorescence which made lipid spots fluorescent under UV. The loaded PL standard and lipid samples with their dilutions (Dilu) are labeled on the bottom. The positions of PL, cholesterol (CHL) and free fatty acids (FFA) spots are marked on the right. Spot intensities were quantified by densitometry, and the percentages of the three components are listed. (B) Superimposed chromatograms of fatty acids from a control rabbit (gray trace) and an FO-fed rabbit (black trace). Peak amplitudes were normalized by the first peak (butylated hydroxytoluene, antioxidant in solvents at 50 ug/ml). The peaks of interest, C20:4,n-6 (arachidonic acid, AA), C20:5,n-3 (eicosapentaenoic acid, EPA) and C22:6,n-3 (docosahexaenoic acid, DHA) are labeled. (C) Data summary. Areas under the peaks of AA, EPA and DHA were normalized by the total areas of peaks above threshold and averaged over three samples from each group. doi:10.1371/journal.pone.0010140.g001

37°C: (1) normal Tyrode's (composition given below), 4–5 min, to monitor the regularity/strength of heart beats, (2) nominally Ca-free Tyrode's supplemented with 0.1% BSA, 6–7 min, to wash out Ca, (3) same solution as (2) but with collagenase (Worthington type II, 0.5 mg/ml), 30 min, to digest the extracellular matrix, and (4) KB solution, 3 min, to stop enzyme action. LV base was minced and the tissue was very gently shaken in KB to release single myocytes. The cell suspension was filtered through a 500- $\mu$ m nylon mesh and stored at room temperature in KB. Experiments were done in  $\leq 8$  hr after cell isolation.

### 3. Patch clamp experiments

Cell suspension was added to a poly-lysine-coated coverslip placed in the bath mounted on an inverted Nikon microscope. After allowing cell attachment for 3–5 min, cells were superfused with normal Tyrode's solution at  $34 \pm 1^\circ\text{C}$ . We used pipettes with tip resistance  $\sim 1\text{--}2$  M $\Omega$ . Patch clamp recordings of whole cell currents were controlled by pClamp 10 via Digidata 1440A, using an Axopatch 200B amplifier. Series resistance was compensated up to 95%. Pipette tip potential was zeroed before making seal, and a liquid junction potential of 10 mV between the pipette and bath solutions (pipette side negative) was corrected during data analysis. Currents were low-pass filtered at 1 kHz (Frequency Devices) and stored for off-line analysis.

### 4. Solutions and drugs

The normal Tyrode's solution contained (mM): NaCl 147, KCl 4, CaCl<sub>2</sub> 2, MgCl<sub>2</sub> 0.5, HEPES 5, dextrose 5.5, pH 7.3

( $\sim 295$  mOsm). The Na- and Ca-free Tyrode's solution was made by equimolar substitution of NaCl and CaCl<sub>2</sub> with choline-Cl and MgCl<sub>2</sub>, respectively, and 25 mM sucrose was added to maintain the osmolarity ( $\sim 302$  mOsm). The pipette solution contained (mM): K-aspartate 110, KCl 20, ATP (K salt) 5, HEPES 5, MgCl<sub>2</sub> 1, pH 7.3 ( $\sim 300$  mOsm). The KB solution contained (mM): K-glutamate 110, KH<sub>2</sub>PO<sub>4</sub> 10, MgSO<sub>4</sub> 1.8, EGTA 0.5, taurine 10, HEPES 10, and glucose 20 ( $\sim 305$  mOsm).

DHA (Sigma) was aliquoted in 10  $\mu$ l volume and stored at  $-80^\circ\text{C}$ . On each experimental day, 1  $\mu$ l of DHA was dissolved in 282  $\mu$ l DMSO to make 10 mM stock solution. The stock solution was kept on ice, and diluted to 10  $\mu$ M in bath solution right before applying to cells. DHA aliquot and stock solution were discarded at the end of each experimental day. Dofetilide was dissolved in water (pH 3) at 1 mM, aliquoted and stored at  $-20^\circ\text{C}$ . It was diluted to 1  $\mu$ M in bath solution right before applying to cells.

### 5. Fatty acid analysis

Lipids were extracted from tissue samples using a procedure modified from that of Folch [8]. All solvents contained butylated hydroxytoluene (BHT, 50  $\mu$ g/ml) to prevent lipid oxidation. Briefly, tissue (0.3–0.7 g) were minced in methanol (6 ml) and homogenized with polytron grinder for 2 min. Chloroform (12 ml) was added and the mixture was further homogenized for 2 min. Then 0.88% (w/v) KCl 4.5 ml was added and the mixture was vortexed vigorously for 2 min. After the phases separated, the lower organic phase was further extracted with 5 ml of methanol plus 0.88% KCl (1:1, v/v). The final organic phase was dried

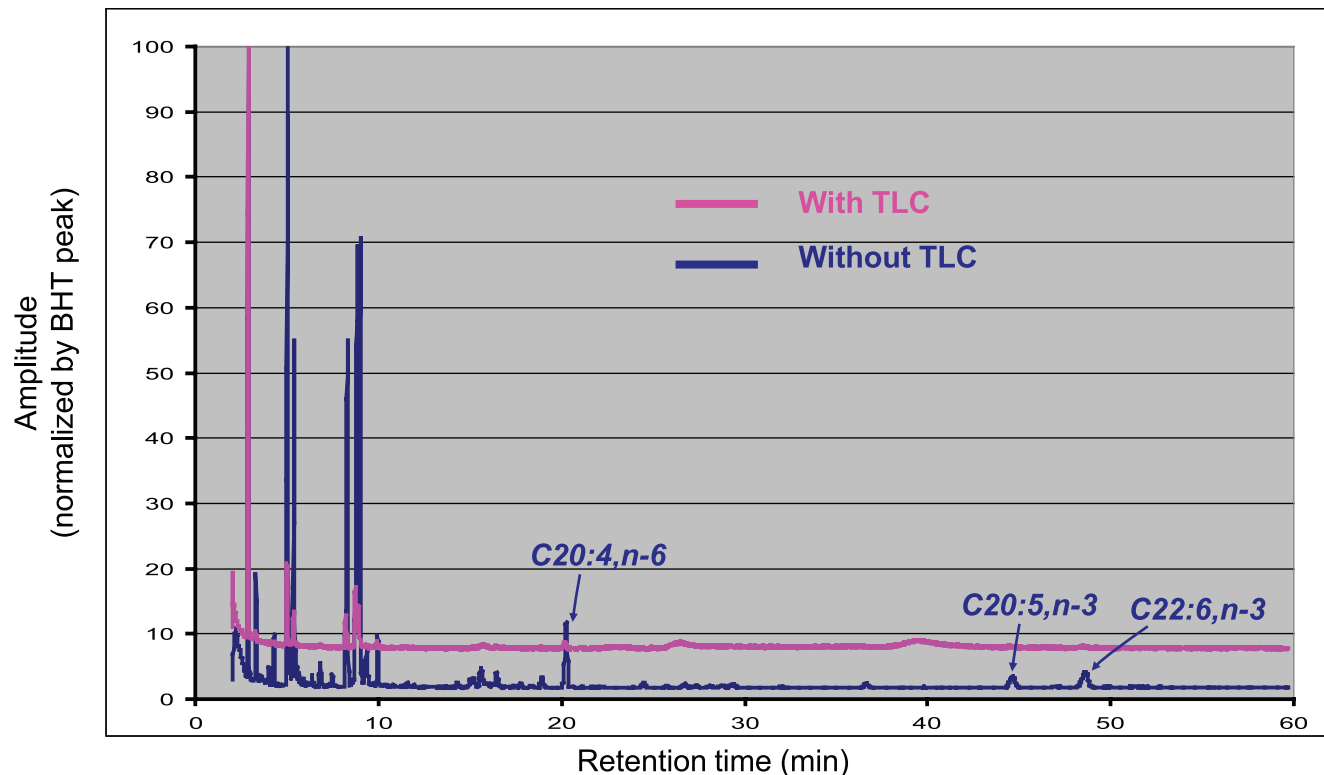


**Figure 2. Effects of the thin-layer chromatography (TLC) procedure on downstream lipid analysis.** Comparing GC-MS chromatograms of transmethylated lipid samples prepared from the same batch of COS-7 cells, with (magenta) or without (dark blue) the TLC procedure to isolate the phospholipid component in the lipids. Peak amplitudes in the retention time range of  $< 10$  min are dramatically reduced after TLC. Importantly, the peaks of long-chain polyunsaturated fatty acids (C20:4,n-6, C20:5,n-3, and C22:6,n-3) are largely missing after TLC, suggesting that the TLC procedures (prolonged exposure to air at elevated temperatures) may have caused extensive oxidation of the polyunsaturated acyl chains, thus invalidating the GC-MS data.

doi:10.1371/journal.pone.0010140.g002

down under a stream of nitrogen, reconstituted in 100  $\mu$ l chloroform and stored at  $-80^{\circ}\text{C}$ .

The phospholipid (PL) component was separated from the other components in the lipid extracts using thin-layer chromatography [9]. Samples along with a PL standard (PL mix from soybean, Supelco) of different dilutions in 10  $\mu$ l total volume were applied to preparative silica gel G plates (20 $\times$ 20 cm, silica gel thickness = 0.5 mm). The mobile phase was hexane/diethyl ether/acetic acid (85:15:1, by vol). After the mobile phase reached within 1 inch to the top, the plate was dried by baking on a hotplate at  $\sim 120^{\circ}\text{C}$  for 5 min, sprayed with 2',7'-dichlorofluorescein (in 95% methanol, 0.1% w/v), and the lipid spots were visualized/quantified under UV (ChemImager model 4400,  $\alpha$ -Innotech).

To make the fatty acids volatile at  $\sim 200^{\circ}\text{C}$  (for separation by gas chromatography), the lipid extracts (25  $\mu$ l) were transmethylated by boiling in excess (500  $\mu$ l) boron trifluoride ( $\text{BF}_3$ , in methanol 14% w/v) in a boiling water bath for 2–3 min. Methyl

esters of long-chain fatty acids were extracted using 1.5 ml hexane/water (3:2, v/v). The organic phase was dried down under a stream of nitrogen, reconstituted in 25  $\mu$ l of hexane and stored at  $-80^{\circ}\text{C}$ .

The above methylated fatty acid samples were analyzed by gas chromatography - mass spectroscopy (GC-MS, Shimadzu, model QP5050A). We used a GC capillary column (Omegawax250, Supelco) designed for the separation of long-chain polyunsaturated fatty acids. The injection volume was 1  $\mu$ l with a split ratio of 30:1. The oven temperature was set a  $200^{\circ}\text{C}$  and the carrier gas (helium) was set at a total flow rate of 1 ml/min. The following methylated fatty acid standards (Supelco) were used to confirm peaks identity: C20:4,n-6, C22:6,n-3, C18:1,n-9, and C18:3,n-3.

## 6. Immunoblot analysis

Except for Kv1.4, the protein levels of channel subunits were quantified from membrane-enriched fraction prepared using

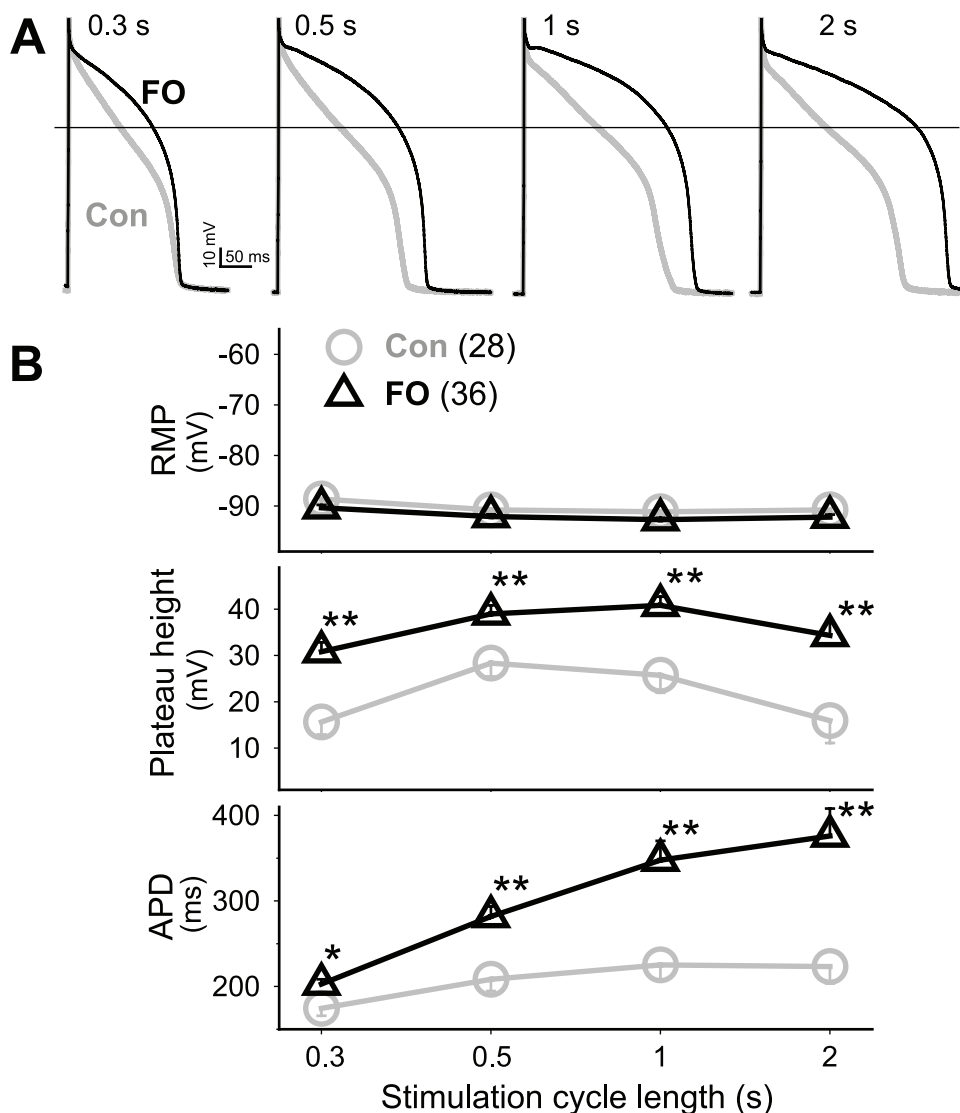


**Figure 3. Fish oil feeding elevated action potential plateau height and prolonged action potential duration in rabbit ventricular myocytes.** (A) Superimposed action potentials recorded from a control (Con) and an FO myocyte at four cycle lengths (marked on top). Horizontal line denotes zero mV. (B) Data summary of RMP (resting membrane potential), plateau height (voltage level 50 ms after the upstroke), and APD (action potential duration, measured when membrane was repolarized to  $-60$  mV). Numbers in parentheses are those of myocytes examined. doi:10.1371/journal.pone.0010140.g003

procedures modified from those described by Takimoto [10]. Frozen tissue chunks were pulverized under liquid nitrogen, and homogenized in 10 vol of buffer (0.25 M sucrose, 1 mM EDTA [pH 7.4]). This and all the following procedures took place in the presence of the protease inhibitor cocktail at 4°C or on ice. The homogenate was centrifuged at 3,500 rpm for 10 min to pellet nuclei and debris. The supernatant was centrifuged at 30,000 rpm for 1 hr to pellet the membranes. The membrane pellet was washed with a solution (Tris-HCl 20 mM [pH 7.4], EDTA 1 mM) and referred to as post-nuclear membrane fraction. The post-nuclear membrane fraction was rehomogenized in a Triton-containing lysis buffer (Tris-HCl 20 mM [pH 7.5], NaCl 0.2 M, EDTA 1 mM, Triton X-100 1%) using Dounce grinder. The mixture was centrifuged at 17,000 rpm for 1 hr, and the supernatant (Triton extract) was used for immunoblotting.

Initial attempts to detect Kv1.4 in the membrane-enriched fraction failed, although the antibody detected a strong ~100 kDa

fuzzy band in whole tissue lysate (WTL) of rat brain (representing glycosylated Kv1.4) and a faint band of a similar size in WTL of rabbit hearts (see below). Therefore, the Kv1.4 data reported here were from WTL prepared using the procedures described by O'Rourke et al [11]. Briefly, frozen tissue chunks were pulverized in 10 vol of lysis buffer (in mM: NaCl 145, MgCl<sub>2</sub> 0.1, HEPES 15, EGTA 10, pH 7, Triton X-100 0.5, with protease inhibitor cocktail), and solubilized for 30 min on ice. The above was homogenized by tip sonicator (2 of 15-s bursts), and then centrifuged to pellet nuclei and debris. The supernatant was used for immunoblotting. Importantly, the effect of FO feeding on Cav1.2 protein measured in the same set of hearts was similar between these two methods of protein preparation (see below).

The protein concentrations in membrane-enriched fraction of WTL were quantified using BCA kit (Pierce). Protein samples were loaded onto 7.5% or 4–20% gradient SDS polyacrylamide gels.

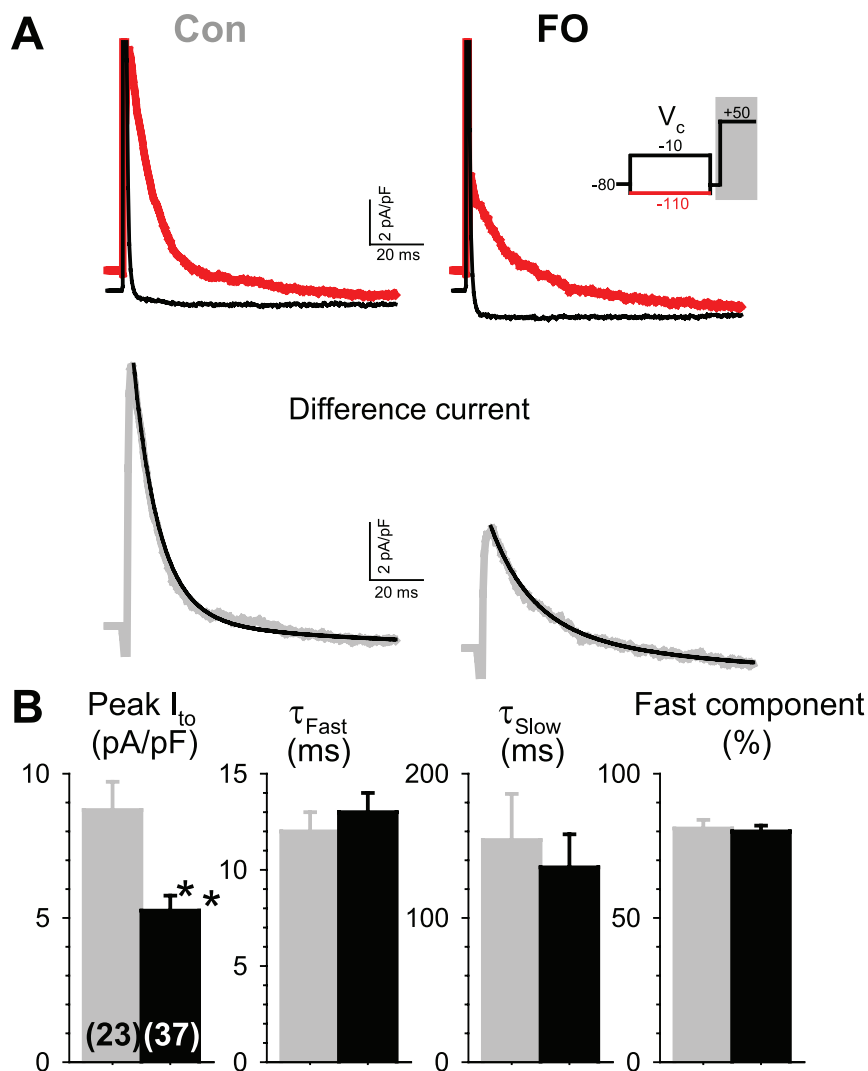


**Figure 4. Fish oil feeding caused a decrease in the peak amplitude of transient outward current ( $I_{to}$ ) in rabbit ventricular myocytes without affecting the time course of  $I_{to}$  inactivation.** (A) *Top*: Superimposed current traces from a control and an FO myocyte using the voltage protocol diagrammed in the inset (showing only currents recorded during the shaded area of the protocol). Red and black traces: currents following a conditioning step ( $V_c$ ) to  $-110$  and  $-10$  mV, respectively. *Bottom*: Difference currents (gray traces). The difference currents were fit with a 2-exponential function (superimposed black smooth curves). (B) Data summary: peak  $I_{to}$  density (left, numbers of myocytes studied listed in parentheses), fast and slow time constants of inactivation ( $\tau_{Fast}$  and  $\tau_{Slow}$ ), and % of the fast component at  $+50$  mV. doi:10.1371/journal.pone.0010140.g004



After fractionation, the proteins were blotted to PVDF membranes (Amersham), and probed with the following antibodies: Cav1.2 - mAb (NeuroMabs), Cav1.1 mAb (Abcam), Kv4.2 pAb (Sigma), Kv4.3 pAb (Alomone), KChIP2 mAb (NeuroMabs), Kv1.4 mAb (NeuroMabs) and hERG pAb (Alomone). Immunoreactivity was visualized using an ECL detection kit (Amersham), and band intensities were quantified by densitometry (ChemImager model 4400). The same membranes were stripped and probed for  $\alpha$ -actin (Sigma) to check loading variations.

## 7. Data analysis

For patch clamp recordings, the experimental protocol and methods of data analysis are described in text or figure legends. Data were analyzed using Clampfit of pClamp10. Statistical analysis of data from patch clamp experiments, GC-MS analysis, and densitometry was done using SigmaStat (v 2.1). Multiple group data were analyzed by one-way ANOVA and, if  $p < 0.05$ , followed by pair-wise comparisons. The t-test was used for comparison between two groups. Statistical significance is noted as: \*\*\*  $p < 0.001$ , \*\*  $p < 0.01$ , \*  $p < 0.05$ .

## Results

### 1. Fish oil feeding enriches n-3 PUFA content in the phospholipids of rabbit heart

Fig. 1A shows that phospholipids (PLs) accounted for  $\geq 90\%$  of the lipids extracted from both control and FO-fed rabbit hearts. To reduce the risk of oxidation of long-chain polyunsaturated acids, which would invalidate the downstream analysis (as shown

in Fig. 2, due to changes in the fatty acid alkyl chain properties), we bypassed the TLC procedure of PL purification and directly subjected lipid extracts to transmethylation and GC-MS analysis.

Fig. 1B shows that we could unequivocally identify C20:4,n-6 (arachidonic acid or AA) and two n-3 PUFA peaks: C20:5,n-3 (eicosapentaenoic acid or EPA) and C22:6,n-3 (docosahexaenoic acid or DHA). FO feeding for 4 weeks markedly increased the content of EPA (from  $0.19 \pm 0.02$  to  $2.96 \pm 0.12\%$ ) and DHA (from  $0.28 \pm 0.05$  to  $4.41 \pm 0.35\%$ ) in rabbit ventricles (Fig. 1C). There was also a slight reduction in AA (from  $16.1 \pm 1.7$  to  $12.0 \pm 0.5\%$ ), although the difference did not reach  $p < 0.05$ .

### 2. Fish oil feeding elevates the action potential plateau voltage and prolongs the action potential duration of rabbit ventricular myocytes

We measured action potential parameters and the following key plateau phase currents in each of the rabbit ventricular myocytes: transient outward ( $I_{to}$ ), L-type Ca ( $I_{CaL}$ ), delayed rectifier ( $I_K$ ), and inward rectifier ( $I_{K1}$ ) currents. To ensure that action potentials and ionic currents were compared among myocytes under similar conditions (i.e., to minimize the issue of current rundown during prolonged whole cell dialysis), after forming the whole-cell recording configuration, all our recordings adhered to the following schedule (time points listed were counted after the formation of whole-cell recording configuration): (1) 0–4 min, allowing whole cell dialysis with the pipette solution and adjusting series resistance compensation, (2) 5–10 min, recording action potentials at 4 cycle lengths (CLs), (3) 10–15 min, recording  $I_{K1}$ ,  $I_{CaL}$ , and  $I_{to}$ , (4) 15–20 min, switching the bath solution from

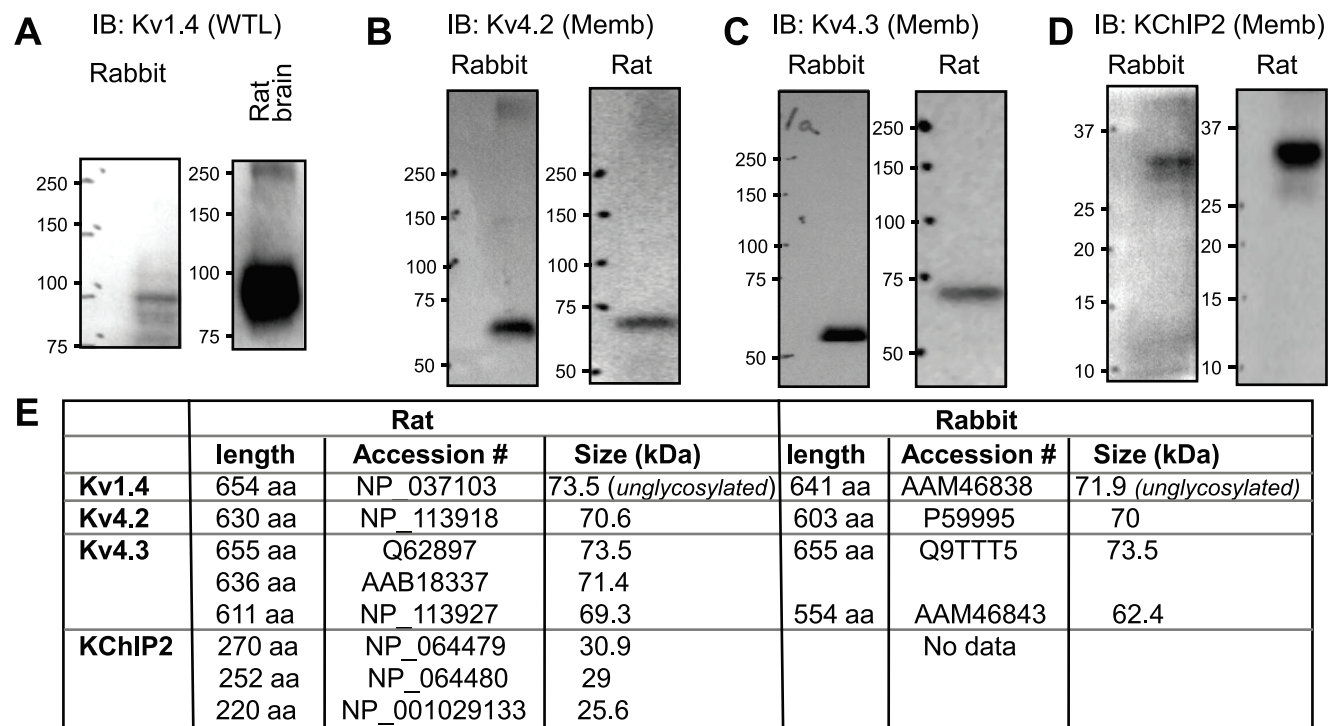


**Figure 5. Validation of Abs used to detect channel subunit proteins in the rabbit hearts.** (A) – (D) Immunoblot images of rabbit and rat hearts (except (A), right lane, rat brain), probed with Abs marked on top. Kv1.4 was detected in whole tissue lysates (WTL), while the other three proteins were detected in membrane-enriched fraction (Memb). (E) Lengths, accession numbers and molecular sizes (in kDa) of rat and rabbit channel subunit orthologs currently available in the NCBI protein database. The Kv1.4 sizes are those of unglycosylated forms, which are smaller than the N-glycosylated forms shown in (A). Kv4.2 and Kv4.3 do not have N-glycosylation signals. The rabbit Kv4.3 we detected (~60 kDa, panel (C), left lane) was likely the short isoform (62.4 kDa). KChIP2 is a cytosolic protein, and thus is not glycosylated.

doi:10.1371/journal.pone.0010140.g005

normal Tyrode's to Na- and Ca-free Tyrode's while monitoring the disappearance of  $I_{Na}$  and  $I_{CaL}$  (to remove interference from  $I_{Na}$ ,  $I_{Ca}$  and Na/Ca exchanger current,  $I_{NCX}$ , in the measurement of  $I_K$ ), (5) 20–25 min, recording  $I_K$ , (6) 25–30 min, washing in dofetilide 1  $\mu$ M while monitoring the change in  $I_K$ , and (6) 30–35 min, recording dofetilide-insensitive currents.

Action potentials were elicited by passing suprathreshold 2-ms current pulses via the patch pipette. We tested the effects of FO feeding on action potential configuration and duration at CLs of 0.3, 0.5, 1 and 2 s, to simulate heart rates of bradycardia - tachycardia. For each of the CLs, a train of action potentials was elicited till the configuration and duration reached a steady state (requiring 36–60 action potentials at the CL of 2 s, 72–120 action potentials at the CL of 0.3 s). The order in which the CLs were applied was random among myocytes to avoid the issues of use-dependent changes in the action potential parameters. The last 10 action potentials of a train were averaged and used to measure the resting membrane potential, the action potential plateau height, and the action potential duration.

Fig. 3A depicts representative APs recorded from a control and an FO myocyte, each subjected to stimulation at 4 CLs. Fig. 3B presents data summary. FO feeding markedly elevated the AP plateau height and prolonged APD at all 4 CLs. The degree of APD prolongation was modest at CL 0.3 s, but became more

profound at longer CLs. On the other hand, FO feeding did not affect the resting membrane potential.

### 3. Fish oil feeding reduces $I_{to}$ current density and $I_{to}$ subunit expression in rabbit ventricular myocytes

We quantified the peak amplitude of  $I_{to}$  at +50 mV to avoid interference from  $I_{Na}$  and  $I_{Ca}$ , because this voltage was close to the apparent reversal potentials of Na and Ca currents. The voltage clamp protocol is diagrammed in the inset of Fig. 4A. From a holding voltage ( $V_h$ ) of -80 mV, a 2-s conditioning pulse to -110 mV was applied to remove  $I_{to}$  inactivation [12], so that a fully available  $I_{to}$  along with other overlapping currents was recorded during the subsequent test pulse to +50 mV (solid trace). Then a 2-s conditioning pulse to -10 mV was applied to maximally inactivate  $I_{to}$  [12], so that a current trace without  $I_{to}$  was recorded during the step to +50 mV (dotted trace). The difference current between the two represents fully available, isolated  $I_{to}$  (lower traces of Fig. 4A). FO feeding decreased the peak  $I_{to}$  current densities from  $8.7 \pm 1.0$  to  $5.2 \pm 0.5$  pA/pF (Fig. 4B, first panel).  $I_{to}$  inactivation followed a double exponential time course (double exponential fits in Fig. 4A, lower panel). FO feeding did not change the time course of  $I_{to}$  inactivation (Fig. 4B, second to fourth panels).

To understand why the  $I_{to}$  peak current density was reduced in FO-fed rabbit ventricle, we used immunoblotting to quantify the

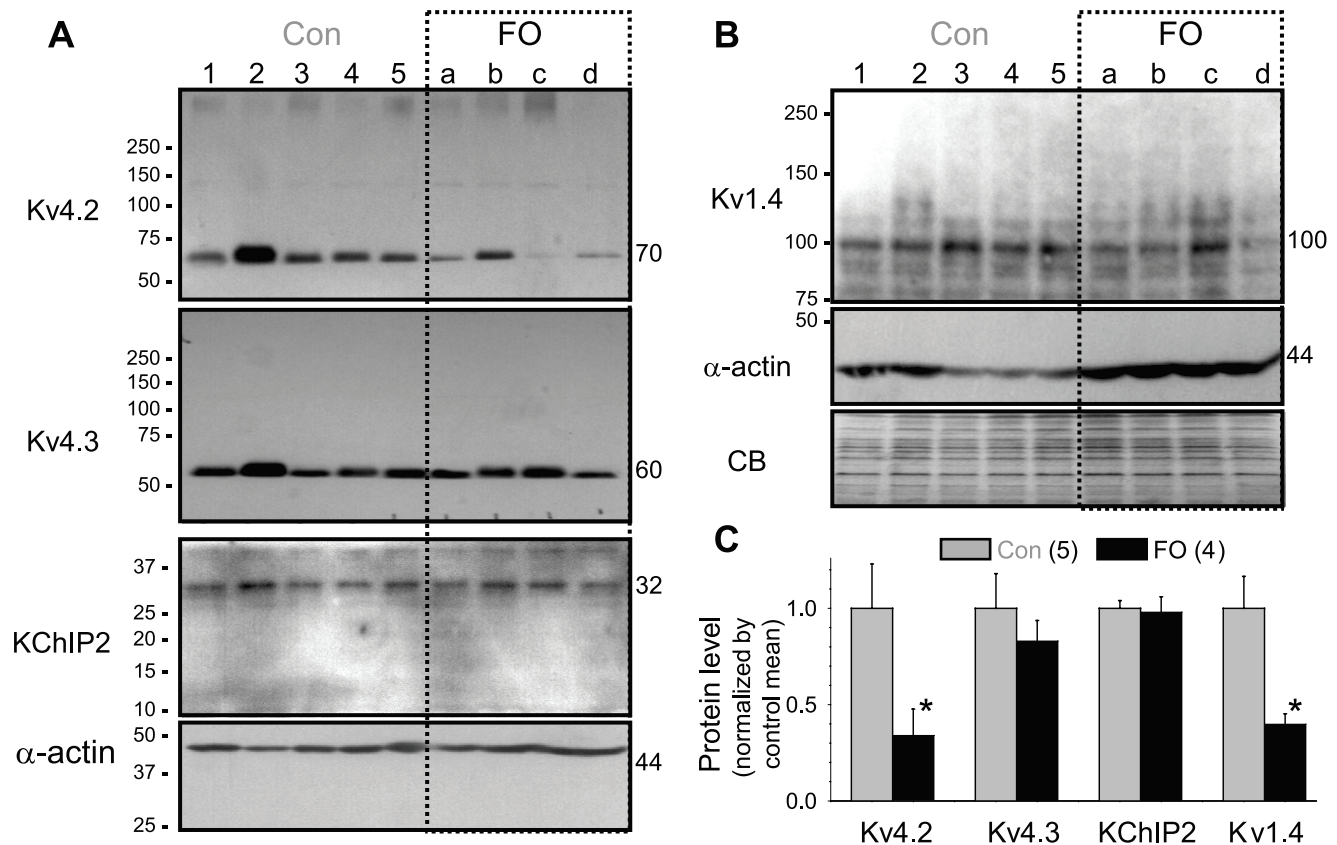


**Figure 6. Fish oil feeding caused a decrease in the protein levels of Kv4.2 and Kv1.4, but not Kv4.3 or KCHIP2, in rabbit ventricles.** (A) Immunoblot images of Kv4.2, Kv4.3, and KCHIP2 (~80  $\mu$ g/lane). (B) Immunoblot images of Kv1.4 (~160  $\mu$ g/lane). Size marker bands (in kDa) are listed on the left. Sizes for proteins of interest are marked on the right. Note that for panel (A) here and Fig. 8A, each channel subunit immunoblot was corrected by its own  $\alpha$ -actin immunoblot for loading variations, although only one representative  $\alpha$ -actin immunoblot is shown. Loading variation in Fig. 6B was further checked by coomassie blue (CB) stain. (C) Data summary: background-subtracted band intensities were divided by corresponding  $\alpha$ -actin band intensity, and then normalized by the mean value of control lanes. doi:10.1371/journal.pone.0010140.g006

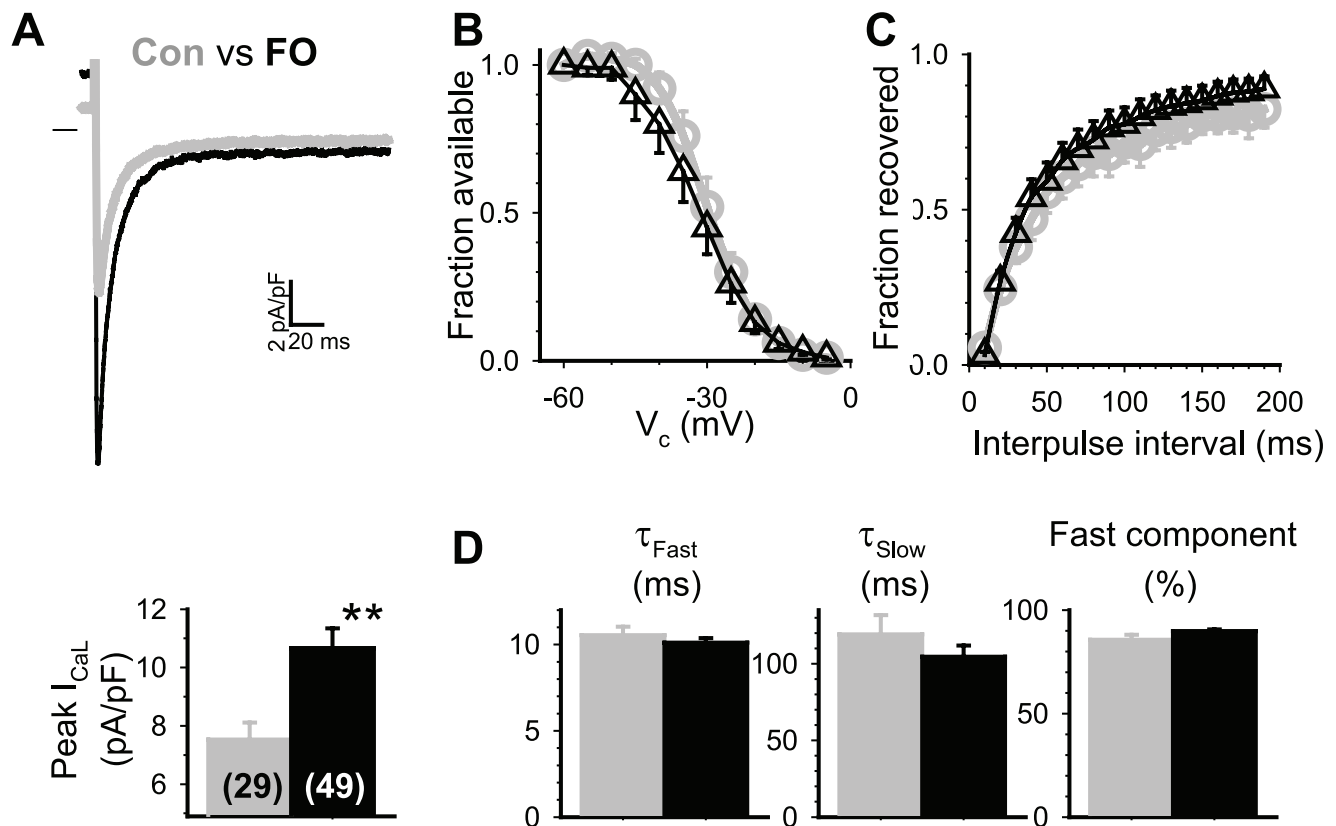
protein levels of  $I_{to}$  channel subunits. Rabbit cardiac  $I_{to}$  has 2 components: Kv4.x-based (Kv4.2 and Kv4.3 as pore-forming subunits, KChIP2 as auxiliary subunit) and Kv1.4-based channels [13]. We used Kv4.2, Kv4.3 and Kv1.4 Abs raised against rat sequences, that are 94%, 98% and 100% identical in rabbit sequences. The KChIP2 Ab was also raised against a rat sequence. We could not find information on rabbit KChIP2 in the NCBI database. Fig. 5 shows validation of these Abs as tools to detect target proteins in the rabbit heart, with rat brain or rat heart proteins as positive controls.

Fig. 6A and 6B depict immunoblot images of  $I_{to}$  channel subunits in five control and four FO-fed rabbit hearts. We used  $\alpha$ -actin as the internal control to correct for variations in protein loading among lanes. Fig. 6C presents data summary of densitometry quantification. Among the four  $I_{to}$  channel subunits examined, Kv4.2 and Kv1.4 protein levels in FO-fed rabbit ventricle dropped to  $0.34 \pm 0.14$  and  $0.40 \pm 0.05$  of control. There was no change in the protein level of Kv4.3 or KChIP2.

#### 4. Fish oil feeding increases $I_{CaL}$ current density and $I_{CaL}$ subunit expression in rabbit ventricular myocytes

We estimated the peak  $I_{CaL}$  by the difference between the inward peak and the current level at the end of a 500 ms pulse from  $V_h$   $-50$  mV to  $0$  mV, where the maximal  $I_{CaL}$  occurred. Representative current traces from a control and an FO myocyte are superimposed in the top panel of Fig. 7A. The maximal peak  $I_{CaL}$  density was markedly increased by FO feeding (from  $7.5 \pm 0.6$  to  $10.7 \pm 0.7$  pA/pF, Fig. 7A, lower panel). We also characterized the voltage-dependence of  $I_{CaL}$  inactivation (Fig. 7B), time course of  $I_{CaL}$  recovery from inactivation at  $-50$  mV (Fig. 7C), and the time course of  $I_{CaL}$  inactivation during depolarization to  $0$  mV (Fig. 7D). FO feeding did not induce any detectable changes in these parameters of  $I_{CaL}$  gating kinetics.

We used immunoblot experiments to test whether there was a corresponding change in the pore-forming subunit of the L-type Ca channels, Cav1.2. The Cav1.2 Ab was raised against a fusion protein containing partial rabbit Cav1.2 sequence (aa 1507–1733).



**Figure 7. Fish oil feeding caused an increase in the peak amplitude of L-type Ca channel current ( $I_{CaL}$ ) in rabbit ventricular myocytes without altering  $I_{CaL}$  gating kinetics.** (A) Top: Superimposed current traces recorded from a control and an FO myocyte. Currents were elicited from a holding voltage ( $V_h$ ) of  $-50$  mV to  $0$  mV. Bottom: summary of peak  $I_{CaL}$  (numbers of myocytes examined in parentheses). (B) Voltage-dependence of inactivation was analyzed using the following protocol. From  $V_h$   $-50$  mV, 2-s conditioning pulses to  $V_c$   $-60$  to  $-5$  mV in  $5$  mV steps were applied. After a 5-ms step to  $-50$  mV to reset the capacitive transient, test pulses to  $0$  mV were used to monitor the availability of  $I_{CaL}$ . Peak amplitudes of  $I_{CaL}$  during the test pulses were normalized by the maximal  $I_{CaL}$  following  $V_c$  to  $-60$  mV, to estimate 'fraction available'. The relationship between 'fraction available' and ' $V_c$ ' was fit with a simple Boltzmann function: fraction available =  $1/[1+\exp((V_c - V_{0.5})/k)]$ , where  $V_{0.5}$  and  $k$  are half-maximum inactivation voltage and slope factor, respectively. The  $V_{0.5}$  and  $k$  values are (mV):  $-29.9 \pm 2.1$  and  $4.5 \pm 0.3$  for control myocytes,  $-32.1 \pm 1.6$  and  $5.3 \pm 0.3$  for FO myocytes. (C) Time course of recovery from inactivation was analyzed using the following protocol. From  $V_h$   $-50$  mV, double pulses each to  $0$  mV for  $500$  ms with varying interpulse interval ( $10$  to  $190$  ms) were applied once every  $10$  s. The peak amplitude of  $I_{CaL}$  during the second pulse was normalized by that during the first pulse to estimate 'fraction recovered'. The relationship between 'fraction recovered' and 'interpulse interval' was fit with a double exponential function. The percentage and time constant of the fast (major) component are  $81 \pm 7\%$  and  $50.2 \pm 4.9$  ms for control myocytes,  $89 \pm 2\%$  and  $55.2 \pm 6.0$  ms for FO myocytes. (D) Time course of  $I_{CaL}$  inactivation at  $0$  mV.  $I_{CaL}$  at  $0$  mV was fit with a double exponential function. Shown are fast and slow time constants of inactivation and % of the fast component. doi:10.1371/journal.pone.0010140.g007



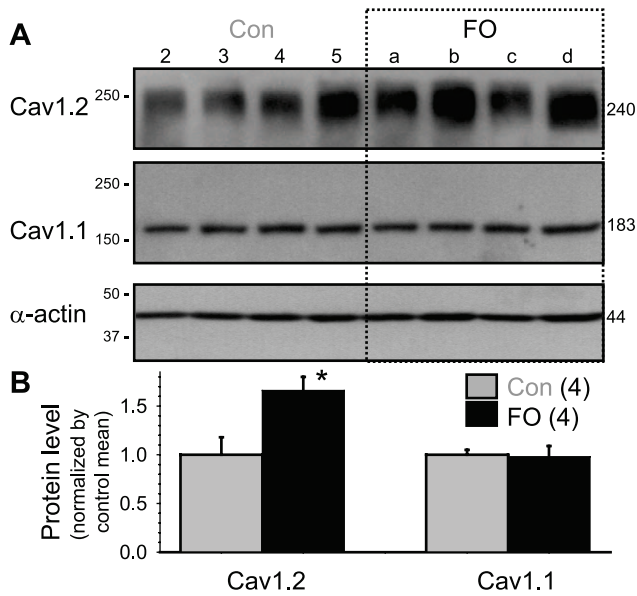


**Figure 8. Fish oil feeding caused an increase in the protein level of Cav1.2, but not Cav1.1, in rabbit ventricles.** (A) Immunoblot images of membrane-enriched fraction from the left ventricular base region of the same set of hearts as shown in Fig. 6 and probed for Cav1.2 and Cav1.1. Loading was  $\sim 80$   $\mu\text{g}/\text{lane}$ . The membranes were stripped and reprobed for  $\alpha$ -actin to check loading. (B) Data summary: background-subtracted and loading-corrected band intensities were normalized by the mean value of control lanes. doi:10.1371/journal.pone.0010140.g008

This Ab recognized a fuzzy band of  $\sim 240$  kDa in rabbit ventricles, as expected for glycosylated Cav1.2. FO-feeding caused a significant increase in Cav1.2 protein level in rabbit ventricles (Fig. 8B,  $1.66 \pm 0.14$  vs  $1.00 \pm 0.18$ ,  $p < 0.05$ ).

Interestingly, a Cav1.1 Ab raised against purified dihydropyridine receptor protein isolated from rabbit skeletal muscle t-tubules could detect a  $\sim 83$  kDa sharp band in rabbit ventricles (Fig. 8).

There was no change in the Cav1.1 protein level in FO-fed rabbit ventricles, supporting the selectivity of FO-feeding in modulating the Cav1.2 protein level.

To check whether the method of sample preparation influenced the results of immunoblot analysis, we compared Cav1.2 quantification in membrane-enriched fraction and in whole-tissue lysate prepared from the same set of hearts. Fig. 9 confirms that immunoblot analysis of both sample preparations reached the same conclusion: FO feeding increased the Cav1.2 protein level in rabbit ventricles.

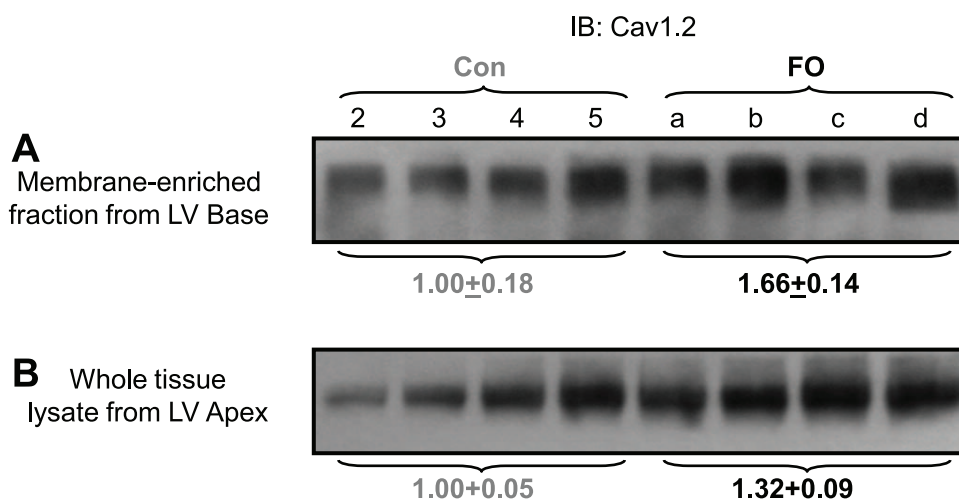
### 5. Fish oil feeding does not affect delayed or inward rectifier current of rabbit ventricular myocytes

Fig. 10A shows that in the presence of dofetilide, little or no outward tail current could be detected in either the control or the FO myocyte. Therefore, under our recording conditions the delayed rectifier ( $I_K$ ) current in rabbit ventricular myocytes was mainly the rapid component ( $I_{Kr}$ ). FO feeding did not affect the  $I_K$  current density or the voltage-dependence of  $I_K$  activation in rabbit ventricular myocytes (Fig. 10B). FO feeding did not alter the protein level of ERG1 ( $\alpha$ -subunit of  $I_{Kr}$  channels) in rabbit ventricles (Fig. 10C). The background current-voltage relationship in the negative voltage range mainly reflects the inward rectifier ( $I_{K1}$ ) current. Fig. 10D shows that FO feeding did not affect  $I_{K1}$  in rabbit ventricular myocytes.

## Discussion

### 1. Molecular mechanisms for fish oil supplementation-induced electrical remodeling

Long-term FO supplementation can affect membrane protein function by at least three mechanisms that are not mutually exclusive. First, incorporation of polyunsaturated acyl chains of  $n-3$  PUFAs into membrane phospholipids will alter the membrane material properties [14]. The increase in membrane fluidity and decrease in lateral pressure may reduce the energy costs of conformational changes in membrane proteins that are critical for their function. Second, an increase in the  $n-3$  PUFA content in the membrane lipid bilayer may facilitate phase



**Figure 9. Fish oil (FO)-feeding induced increase in Cav1.2 protein level was similarly seen in both membrane-enriched fraction and in whole tissue lysate prepared from the same set of hearts.** The immunoblot image in (A) was the same as that shown in Fig. 8A, top panel. Immunoblot in (B) was from the same PVDF membrane as shown in Fig. 6B, top panel (Kv1.4 immunoblot). The PVDF membrane was stripped of Kv1.4/secondary Abs, and reprobed with the Cav1.2 mAb. Numbers shown below the immunoblots are Mean  $\pm$  SE values of background-subtracted/loading-corrected band intensities normalized by the mean values of control lanes. In both cases,  $p < 0.05$ , FO vs control (Con). doi:10.1371/journal.pone.0010140.g009

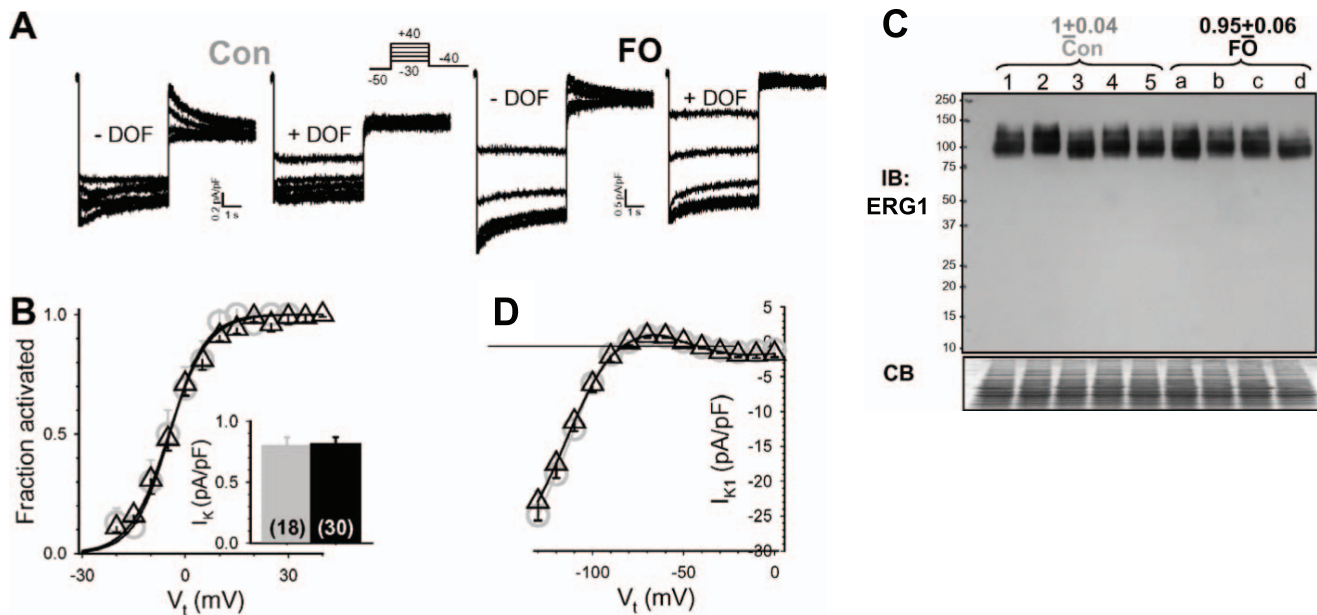


**Figure 10. Fish oil feeding did not alter the delayed rectifier ( $I_K$ ) or inward rectifier ( $I_{K1}$ ) current in rabbit ventricular myocytes.** (A) Representative current traces recorded from a control and an FO myocyte, before and during exposure to 1  $\mu$ M dofetilide (DOF). *Inset*: protocol ( $V_h$   $-50$  mV,  $V_t$  to  $-30$ – $+40$  mV in 5 mV steps for 5 s,  $V_t$  to  $-40$  mV for 5 s, interpulse interval 30 s). (B) Summary of voltage dependence of  $I_K$  activation (*main graph*) and  $I_K$  current amplitude (*inset*). The voltage-dependence of activation was analyzed by normalizing the  $I_K$  tails to the maximal  $I_K$  tail following  $V_t$  to  $+40$  mV (fraction activated), and the relationship between 'fraction activated' and ' $V_t$ ' was fit with a Boltzmann function: fraction activated =  $1/[1+\exp((V_{0.5}-V_t)/k)]$ , where  $V_{0.5}$  and  $k$  are half-maximum activation voltage and slope factor, respectively. The  $V_{0.5}$  and  $k$  values are (mV):  $-4.5\pm 2$  and  $5.2\pm 1.0$  for control myocytes,  $-4.7\pm 1.2$  and  $5.6\pm 0.4$  for FO myocytes. The  $I_K$  current amplitude was measured from peak tail current following  $V_t$  to  $+40$  mV (numbers of cells analyzed in parentheses). (C) Immunoblot analysis of ERG1 protein level in control and FO rabbit LV (same set of hearts as shown in Figs. 6 and 8). Shown on top are Mean  $\pm$  SE of ERG1-immunoreactive band intensities corrected for loading (divided by CB stain) and normalized by the mean value of control rabbits ( $p=0.524$ ). (D) Background current-voltage relationship was analyzed using the following voltage clamp protocol. From  $V_h$   $-50$  mV, test pulses to  $V_t$  of 0 to  $-120$  mV in 10 mV steps for 500 ms were applied once every 5 s. Currents were measured at the end of the test pulses. doi:10.1371/journal.pone.0010140.g010

separation between PUFA-rich/sphingomyelin and cholesterol-poor disordered lipid domains and PUFA-poor/sphingomyelin and cholesterol-rich ordered lipid domains (lipid rafts) [15]. This can lead to changes in the function and modulation of membrane proteins associated with lipid rafts [16]. Third, PUFAs can modulate gene expression [17] by regulating the activity of transcription factors directly (e.g. steroid regulatory element-binding proteins) or indirectly by binding to nuclear receptors (e.g. peroxisome proliferators-activated receptors) [18]. Our observations that long-term FO feeding altered  $I_{CaL}$  and  $I_{to}$  channel subunit expression in rabbit hearts suggest that the third mechanism, altered gene expression, is at work.

## 2. Chronic effects of fish oil supplementation vs acute effects of n-3 PUFAs

Fig. 11 shows that acute application of n-3 PUFA (DHA, 10  $\mu$ M) markedly suppressed the peak amplitudes of  $I_{CaL}$  and  $I_{to}$  in rabbit ventricular myocytes. These observations are similar to previous reports of tissue bath experiments [5,19]. Acute effects of n-3 PUFAs on membrane channels in the heart are likely to occur in vivo transiently after ingestion of FO, when the plasma level of n-3 PUFAs is high. Importantly, the effects of chronic FO feeding on  $I_{CaL}$  (enhancement) differ from that of acute DHA application (suppression), while both treatments similarly suppress the  $I_{to}$  amplitude. Based on these observations, we suggest that dietary FO supplementation in humans will have both chronic (sustained) and acute (transient) effects, and the two aspects may antagonize or complement each other.

## 3. Clinical Implications

We show that ventricular myocytes isolated from FO-fed rabbits, relative to myocytes from control rabbits, had much more positive plateau heights and longer action potential durations tested at cycle lengths of 0.3–2 s. Our observations were consistent

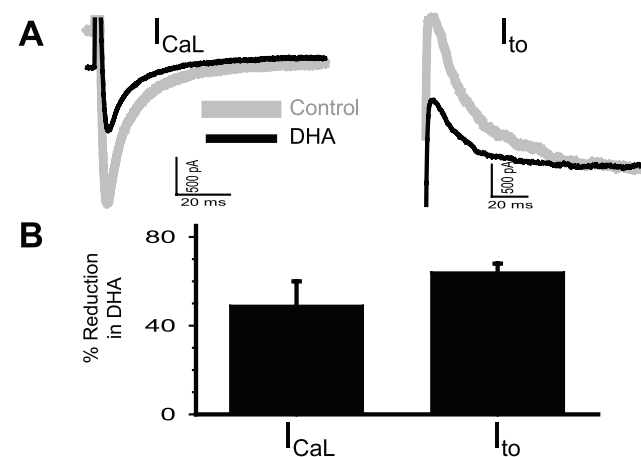


**Figure 11. Effects of acute exposure to DHA (10  $\mu$ M) on  $I_{CaL}$  and  $I_{to}$  in rabbit ventricular myocytes.**  $I_{CaL}$  and  $I_{to}$  were measured as described for Fig. 7A and Fig. 4A, respectively, before and during exposure to DHA. (A) Superimposed current traces. (B) Summary of % reduction of peak  $I_{CaL}$  and  $I_{to}$  in DHA. doi:10.1371/journal.pone.0010140.g011

with a previous report showing that FO feeding in rabbits for 30 days caused a prolongation of the plateau phase of monophasic action potentials recorded from the ventricles of Langendorff-perfused hearts [20].

Our observations are different from a previous study in the pig model [7]. FO feeding in pigs caused a decrease in action potential plateau height and a shortening of APD. These changes were accounted for by a decrease in  $I_{CaL}$  and  $I_{NCX}$ , along with an increase in the slow delayed rectifier ( $I_{Ks}$ ) and  $I_{K1}$  [7]. The differences in FO feeding-induced cardiac electrical remodeling between rabbit and pig models may be due to a combination of factors: differences in cellular and membrane environment of ion channels in cardiac myocytes which can impact the effects of n-3 PUFA enrichment, differences in gene regulation, and differences in the animal diets. These species variations serve as a cautionary note about generalizing animal studies to the clinical situation.

## References

- London B, Albert C, Anderson ME, Giles WR, van Wagoner DR, et al. (2007) Omega-3 fatty acids and cardiac arrhythmias: prior studies and recommendations for future research: a report from the National Heart, Lung, and Blood Institute and Office of Dietary Supplements Omega-3 Fatty Acids and their Role in Cardiac Arrhythmogenesis Workshop. *Circulation* 116: e320–e335.
- Marchioli R, Barzi F, Bomba E, Chieffo C, Di Gregorio D, et al. (2002) Early protection against sudden death by n-3 polyunsaturated fatty acids after myocardial infarction: time-course analysis of the results of the Gruppo Italiano per lo Studio della Sopravvivenza nell'Infarto Miocardico (GISSI)-Prevenzione. *Circulation* 105: 1897–1903.
- Xiao Y-F, Sigg DC, Leaf A (2005) The antiarrhythmic effect of n-3 polyunsaturated fatty acids: modulation of cardiac ion channels as a potential mechanism. *J Memb Biol* 206: 141–154.
- Xiao Y-F, Kang JX, Morgan JP, Leaf A (1995) Blocking effects of polyunsaturated fatty acids on  $Na^+$  channels of neonatal rat ventricular myocytes. *PNAS* 92: 11000–11004.
- Xiao Y-F, Gomez AM, Morgan JP, Lederer WJ, Leaf A (1997) Suppression of voltage-gated L-type  $Ca^{2+}$  currents by polyunsaturated fatty acids in adult and neonatal rat ventricular myocytes. *PNAS* 94: 4182–4187.
- Xiao Y-F, Ke Q, Wang S-Y, Auktor K, Yang Y, et al. (2001) Single point mutations affect fatty acid block of human myocardial sodium channel  $\alpha$  subunit  $Na^+$  channels. *PNAS* 98: 3606–3611.
- Verkerk AO, van Ginneken ACG, Berecki G, Den Ruijter HM, Schumacher CA, et al. (2006) Incorporated sarcolemmal fish oil fatty acids shorten pig ventricular action potentials. *Cardiovasc Res* 70: 509–520.
- Folch J, Lees M, Sloane-Stanley GH (1957) A simple method for the isolation and purification of total lipids from animal tissues. *J Biol Chem* 226: 497–509.
- Christie WW (1989) Fatty acids and lipids: structures, extraction and fractionation into classes. In: Christie WW, ed. *Gas Chromatography and Lipids, A Practical Guide* Bridgewater: Oily Press. pp 5–23.
- Jia Y, Takimoto K (2006) Mitogen-activated protein kinases control cardiac KChIP2 gene expression. *Circ Res* 98: 386–393.
- O'Rourke B, Kass DA, Tomaselli GF, Kaab S, Tunin R, et al. (1999) Mechanisms of altered excitation-contraction coupling in canine tachycardia-induced heart failure. I. Experimental studies. *Circ Res* 84: 562–570.
- Rose J, Armondas AA, Tian Y, DiSilvestre D, Burysek M, et al. (2005) Molecular correlates of altered expression of potassium currents in failing rabbit myocardium. *Am J Physiol* 288: H2077–H2087.
- Wickenden AD, Tsushima RG, Losito VA, Kaprielian R, Backx PH (1999) Effect of  $Cd^{2+}$  on Kv4.2 and Kv1.4 expressed in *Xenopus* oocytes and on the transient outward currents in rat and rabbit ventricular myocytes. *Cellular Physiology and Biochemistry* 9: 11–28.
- Bruno JJ, Koeppel REII, Andersen OS (2007) Docosahexaenoic acid alters bilayer elastic properties. *PNAS* 104: 9638–9643.
- Wassall SR, Brzustowicz MR, Shaikh SR, Cherezov V, Caffrey M, et al. (2004) Order from disorder, corralling cholesterol with chaotic lipids. The role of polyunsaturated lipids in membrane raft formation. *Chemistry and Physics of Lipids* 132: 79–88.
- Stulnig TM, Huber J, Leitinger N, Imre E-M, Angelisova P, et al. (2001) Polyunsaturated eicosapentaenoic acid displaces proteins from membrane rafts by altering raft lipid composition. *J Biol Chem* 276: 37335–37340.
- Pepe S (2005) Effect of dietary polyunsaturated fatty acids on age-related changes in cardiac mitochondrial membranes. *Experimental Gerontology* 40: 369–376.
- Edwards IJ, O'Flaherty JT (2008) Omega-3 fatty acids and PPAR $\gamma$  in cancer. *PPAR Research* 2008: 358052.
- Bogdanov KY, Spurgeon HA, Vinogradova TM, Lakatta EG (1998) Modulation of the transient outward current in adult rat ventricular myocytes by polyunsaturated fatty acids. *Am J Physiol* 274: H571–H579.
- Dujardin KS, Dumotier B, David M, Guizy M, Valenzuela C, et al. (2008) Ultrafast sodium channel block by dietary fish oil prevents dofetilide-induced ventricular arrhythmias in rabbit hearts. *Am J Physiol* 295: H1414–H1421.

They also suggest that the effects of FO supplementation on the cardiac electrical activity in people can vary due to differences in genetic make-up and conditions of the heart.

## Acknowledgments

We thank Dr. Joseph Feher (Dept. Physiology & Biophysics, Virginia Commonwealth University) and Dr. Linda Boland (Dept. Biology, University of Richmond) for their kind assistance in setting up the lipid extraction and GC-MS experiments.

## Author Contributions

Conceived and designed the experiments: GNT. Performed the experiments: XX MJ YW GNT. Analyzed the data: XX MJ YW GNT. Contributed reagents/materials/analysis tools: TS CMB MAW. Wrote the paper: GNT.